Natural Resources for Human Health
eISSN: 2583-1194

Original Research

Received 18 May 2026
Revised 28 June 2026
Accepted 18 July 2026

Natural Resources for Human Health 2026, Vol. 6 (8s): 396–407

KEYWORDS:
Climate Variability; Himalayan Foothills; Mann–Kendall Test; Sen's Slope Estimator; Agro-pastoral Livelihoods; Jammu and Kashmir

Seasonal Climate Asymmetry and Livelihood Impacts in Kathua, Himalayan Foothills (1990-2024)

Jyotirupa Devi and Juhi Gupta

Department of Climate Change and Environmental Sustainability, Amity Institute of Environment and Sustainability, Amity University, Noida, Uttar Pradesh, India
Emails: jyotirupa.devi@s.amity.edu (corresponding author); jgupta2@amity.edu

ABSTRACT: The densely populated agrarian and agro-pastoral communities of the Himalayan foothills are extremely sensitive to seasonal climate changes. This research analyses trends in temperature and rainfall for the month, season, and year in the Kathua district of Jammu and Kashmir, India, from 1990 to 2024 using India Meteorological Department gridded data. The Mann–Kendall test procedure with the Hamed–Rao autocorrelation correction and Sen's slope estimator is used for this study. The mean temperature over the years shows a small, statistically non-significant increasing trend of 0.012 °C yr^{-1} ($p = 0.16$ during the study period), resulting in a change of 0.4 °C. The overall average value presented hides a strong seasonal asymmetry: August (0.019 °C yr^{-1}; $p = 0.047$) and September (0.029 °C yr^{-1}; $p < 0.05$) exhibit a significant warming, whereas December shows statistically significant cooling under the autocorrelation-corrected test (–0.020 °C yr^{-1}; $p = 0.018$). The average annual rainfall across the years is 1417 mm, exhibiting a 19.5% coefficient of variation. No significant trend is detected in any month, season or year, but there is a high degree of interannual variability. Annual totals have ranged from 785mm (2002) to 1886mm (1995). The district's climate hazard exposure appears to be concentrated in the late monsoon agricultural calendar rather than in mean annual change. This has direct ramifications for thwarting kharif harvesting, rabi sowing and agro-pastoral adaptation planning.

INTRODUCTION

The rate of climate change in High Mountain Asia is faster than global averages. Climate change consequences in High Mountain Asia are cascading through the region. The populations most affected by the consequences of Climate change in High Mountain Asia include the 2 billion people dependent on the waters of the Hindu Kush Himalaya (Immerzeel et al., 2020; Wester et al., 2019; ICIMOD, 2023). As per IPCC (2021), there is high confidence that surface warming over Asia has already exceeded 1°C (with respect to pre-industrial levels), and that monsoon precipitation over South Asia will become more variable through the twenty-first century, with higher extremes, even where changes in mean totals remain modest. India, specifically, the national climate assessment indicates a rise of approximately 0.7°C in mean annual temperature over 1901–2018, along with a strong increase in the frequency of localised heavy rainfall events and a weakening of mean summer monsoon rainfall (Krishnan et al., 2020). Though there are continental-scale signals, regional topography, circulation, and land-atmosphere feedbacks mediate these signals. The direction, magnitude, and seasonality of change at the district scale cannot thus simply be read off national assessments. Adaptation planning is actually implemented at this scale in India.

The northwestern Himalaya showed unique regional signals in this continental picture. Long instrumental records show statistically significant warming in the twentieth century, driven disproportionately by rising maximum temperatures rather than minimum temperatures (Bhutiyani et al., 2007). Precipitation shows quite strong inter-decadal variability with a diminishing monsoon component since the mid-twentieth century (Bhutiyani et al., 2010). The Jammu, Kashmir, and Ladakh region has witnessed a significant decline in the ecological and hydrological impacts of winter precipitation, largely due to a reduction in the frequency of western disturbances embedded in the subtropical westerly jet. Guhathakurta & Rajeevan (2008). Recent studies on the Kashmir region have reported a warming trend of about 0.8 degrees Celsius over the period 1980-2016, mostly concentrated in winter and spring months (Zaz et al., 2019). Similarly, station and gridded analyses of the Jhelum basin were extended till 2023 and confirmed warming trends with a significant seasonal structure (Hamid & Samantaray, 2025). According to a 2021 study by Dad and others, time-series analysis of the Kashmir Himalaya depicts warming accompanied by heterogeneous precipitation change. The region is experiencing real, seasonal, and unevenly distributed climate change.

Despite hosting denser agricultural populations and functioning as the first receiving zone for both monsoon depressions and winter westerlies, the outer Himalayan foothills, the Shiwalik belt, where mountain and plain economies meet, is less studied than the Kashmir valley or the high Himalaya. Warming documented across the Hindu Kush Himalaya (Wester et al., 2019) means valley-floor and foothill trajectories cannot be assumed to be similar to those of high-altitude stations. Also, the use of gridded data for the northwestern Himalaya cautions that trends derived for one physiographic zone do not transfer well to another. The only previous trend study of Kathua district itself, covering conference analysis for 1985-2010, indicates rising minimum temperatures and shifting monthly rainfall (Singh et al., 2021), which is based on data from the recent decade and a half and did not address serial correlation for the tested series.

The gap in question is important for human geography, not just climatology. The economic structure of Kathua is based on kharif paddy and maize, which mainly depend on rainfall. Rabi wheat is also cultivated in the area. Moreover, the Gujjar and Kankwal communities engage in transhumant pastoralism, migrating seasonally between the plains and high pasture, which are set according to the monsoon calendar (Mir & Batool, 2022). The seasonal climate mostly determines livelihood systems rather than annual means (Negi et al., 2017; Negi et al., 2012). Perception-based studies across the western Himalaya show that farmers consistently report month-specific changes (late winter rains and warmer harvest windows) long before annual statistics register a trend. A trend analysis that breaks down data by month and season, is statistically robust to serial correlation, and provides a reliable method for detecting false trends in climatic series, was a condition for locally grounded adaptation planning under the Sustainable Development Goals.

In light of this, the present study asks three questions. What are the monotonic trends that characterise the monthly, seasonal, and annual temperatures and rainfall in the Kathua district? The second aspect that needs to be interrogated concerns whether trends are symmetrical seasonally or concentrated in some part of the annual cycle. In the third place, what does the observed pattern imply for the agrarian and agro-pastoral livelihood calendar of the district and for the design of adaptation responses? To address these questions, the research provides a robust district-scale climatology that accounts for autocorrelation and explicitly links the statistical findings to the human systems they influence.

STUDY AREA

Kathua district (approximately 32°17'–32°55' N, 75°70'–76°16' E is situated at the southernmost margin of the Union Territory of Jammu and Kashmir. The area ascends from the Punjab plains through the Shiwalik foothills to the Pir Panjal range. The Punjab borders it to the southeast, Himachal Pradesh to the northeast, Udhampur and Doda districts to the north and northwest, Jammu district to the west, and, above all, it has an international border with Pakistan to the southwest. The district covers 2502 km² and has a population of 0.62 million (Census of India, 2011). The district is drained by the Ravi and its tributaries, the Ujh and the Sewa. Climatic gradients ranging from humid subtropical in the plains to temperate in the Bani-Basohli uplands are driven by elevation. Of the total annual rainfall, approximately 62% occurs during the summer monsoon season (June-September). A further 18% is received in the winter (December-February) from western disturbances. This rainfall pattern is indicative of the dual precipitation regime of the northwestern Himalayan foothills. Rural livelihoods mainly comprise agriculture, horticulture, and livestock rearing, and the district lies on the seasonal migration corridors of Gujjar-Bakarwal pastoralists between the outer plains and the alpine pastures (Mir & Batool, 2022).

Natural Resources for Human Health
eISSN: 2583-1194

Fig. 1 Location of Kathua district, Union Territory of Jammu and Kashmir, India.

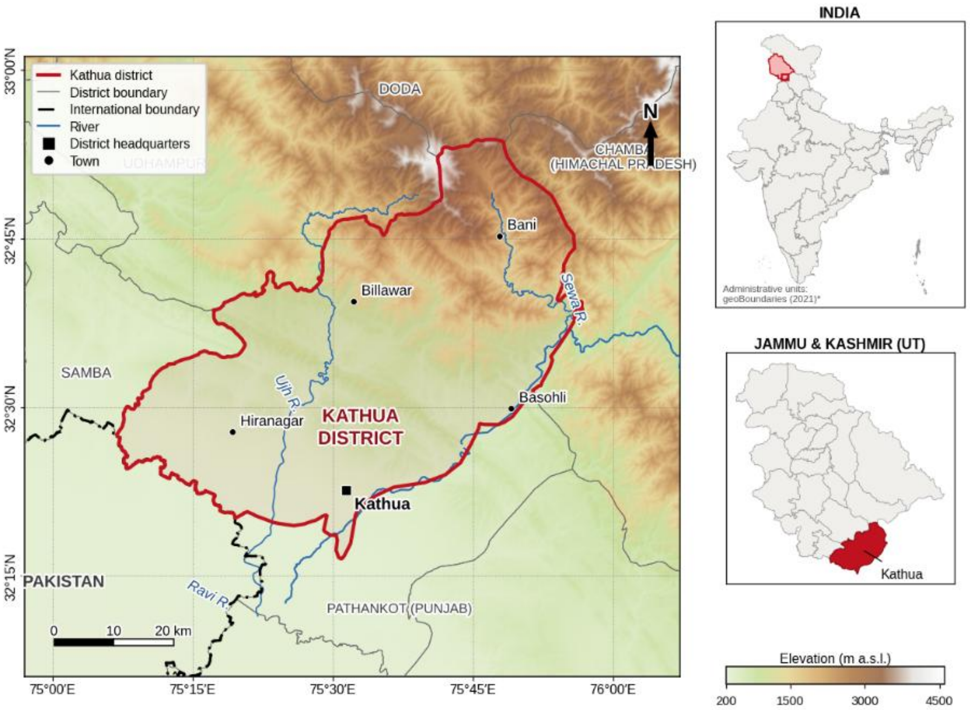

Source: Map prepared in Python 3 using GeoPandas and Matplotlib. Administrative boundaries: geoBoundaries gbOpen (2021); elevation: SRTM via Mapzen/AWS Terrain Tiles; drainage: © OpenStreetMap contributors (ODbL). *Note:* Main panel: relief, drainage (Ravi, Ujh and Sewa rivers), administrative boundaries and principal settlements; insets show the position of J&K within India and of Kathua within the Union Territory.

Data

During the period of January 1990 to December 2024, the maximum and minimum temperature were provided in all the days gridding at a 1°×1° resolution (Srivastava et al., 2009) and daily gridded rainfall 0.25° × 0.25° resolution (Pai et al., 2014) both produced by India Meteorological Department (IMD), were extracted using open-source IMDLIB library (Nandi et al., 2024). The average of the daily maximum and minimum temperatures at the grid point (32.5°N, 75.5°E) covering the district was used to represent the daily mean temperature. Averaged over all 0.25° grid cells within 32.25-33.0° N and 75.25-76.25° E (i.e. the bounding box of the district); a district-average series is preferred because point selections on individual cells in complex terrain run the risk of including cells outside the study unit. Monthly means (temperature) and monthly totals (rainfall) were generated from daily values, and four seasons were created as per IMD convention with slight modification to the regional calendar: winter (December–February), summer (March–May), monsoon (June–September) and post-monsoon (October–November). The annual temperature and rainfall of a headquarters station shall be computed on the basis of mean monthly values and total yearly precipitation, respectively. The winter seasonal series refers to December of the same calendar year.

METHODS

The Mann-Kendall test (MK) was used to assess the direction and significance of the trends. The MK test is recommended by the World Meteorological Organisation for hydroclimatic series because it does not require assumptions about the underlying distribution and is robust to outliers and missing values (Mann, 1945; Kendall, 1975). The MK test determines whether a dataset exhibits a monotonic trend. The null hypothesis (H_0) states that there is no monotonic trend, while the alternative hypothesis (H_1) indicates that the dataset does exhibit a monotonic trend. The statistic designated S is calculated as

$$S = \sum_{k=1}^{n-1} \sum_{j=k+1}^{n} sgn(x_j - x_k) \qquad (1)$$

where n is the length of the series and the sign function is defined as

$$sgn(\theta) = \{ +1\, if\ \theta > 0;\ 0\, if\ \theta = 0;\ -1\, if\ \theta < 0 \} \quad (2)$$

A positive S indicates an increasing tendency and a negative S a decreasing tendency. For n ≥ 10 the statistic is approximately normally distributed with variance

$$Var(S) = \frac{n(n-1)(2n+5) - \sum_{i=1}^{m} t_i(t_i-1)(2t_i+5)}{18} \quad (3)$$

where m is the number of tied groups and t_i the number of observations in the i-th tied group. The standardised test statistic is

$$Z = \frac{S - sgn(S)}{\sqrt{Var(S)}} \quad (4)$$

When the absolute value of [Z] exceeds the respective critical value of the standard normal distribution, the null hypothesis is rejected at significance level α. Due to positive serial correlation, which increases the variance of S and thus leads to false trend detection, all tests were also performed by correcting the variance as described by Hamed and Rao (1998), which scales Var(S) by a factor derived from the significant autocorrelation coefficients of the ranked, detrended series. We report results as "significant" only if they pass the corrected test, unless otherwise indicated.

The magnitude of the trend was quantified with the non-parametric slope estimator of Sen (1968),

$$Q = median\frac{x_j - x_k}{j - k},\ j > k \quad (5)$$

In this context, x_j and x_k represent the values of the data at time j and k (j > k), and the median is calculated over all the N = n(n − 1)/2 pairwise slopes. Q sign indicates the orientation of the trend while its value stands for the steepness. To characterize variability, we computed descriptive statistics, including the mean, standard deviation (SD), coefficient of variation (CV), minimum, and maximum. The pymannkendall library in Python 3.12 was used for all computations at a significance level of α = 0.05.

RESULTS AND DISCUSSION

Temperature

The interannual statistics of monthly, seasonal and annual mean temperature are presented in table 1. The highest interannual variation is observed during the winter and spring months (SD 0.94–1.73 °C; February CV 12.8%). This is due to the irregularities of western disturbance activity from one year to another. While the least interannual variation occurs during the core monsoon months (July–September, SD ≤ 0.67 °C). The massive cloud cover and the exchange of latent heat act as a buffer for surface temperature during this period. The seasonal differences in variability are significant geographically. The winter climate in the foothills is the least predictable element of the annual cycle. The monsoon thermal regime, however, is more stable from year to year.

Table 1 Descriptive statistics of monthly, seasonal, and annual mean temperature (°C), Kathua district, 1990–2024 (interannual statistics of the monthly-mean series, n = 35)

Period	Min	Max	Mean	SD	CV (%)
January	6.19	10.96	9.26	0.98	10.5
February	8.04	16.14	11.88	1.52	12.8
March	12.91	19.85	16.19	1.73	10.7
April	17.44	25.04	21.37	1.57	7.4
May	22.66	27.71	25.41	1.25	4.9
June	25.65	29.43	27.37	0.85	3.1
July	25.68	28.10	26.82	0.55	2.1
August	24.37	27.03	26.18	0.57	2.2

Period	Min	Max	Mean	SD	CV (%)
September	23.04	25.98	24.63	0.67	2.7
October	18.53	22.16	20.73	0.81	3.9
November	14.17	16.95	15.63	0.70	4.5
December	8.28	13.10	11.17	0.94	8.4
Winter (DJF)	7.51	12.37	10.77	0.90	8.4
Summer (MAM)	17.96	23.76	20.99	1.22	5.8
Monsoon (JJAS)	24.93	26.99	26.25	0.41	1.6
Post-monsoon (ON)	16.35	19.35	18.18	0.64	3.5
Annual	17.54	20.58	19.72	0.59	3.0

Table 2 shows the results of the Mann-Kendall and Sen's slope analyses at seasonal and annual scales. Table 3 shows the results at monthly scale. At yearly scale mean temperature shows an upward but statistically non-significant trend (Sen's slope 0.012 °C yr^{-1}; p=0.164) approximately equal to 0.4 °C during the 35-year window (Fig. 2). The warming of foothills is less than 0.8 °C, the estimated warming in Kashmir valley by Zaz et al. (2019) for a similar time frame. The climatic influence of irrigation and monsoon cloudiness could be a reason for this lower warming. This lowest warming in Kashmir valley is also in line with the elevation-dependent warming of the Hindu Kush Himalaya (Wester et al. 2019). There is no trend in any of the four seasons while in the monsoon season effect is approaching significance (p = 0.065).

Table 2 Mann–Kendall and Sen's slope results for seasonal and annual mean temperature, 1990–2024

Statistic	Winter	Summer	Monsoon	Post-monsoon	Annual
Kendall's tau	0.042	0.079	0.220	0.025	0.166
S	25	47	131	15	99
p (original)	0.733	0.514	0.065	0.842	0.164
p (Hamed–Rao)	0.640	0.514	0.065	0.842	0.164
Sen's slope (°C yr^{-1})	0.006	0.014	0.011	0.003	0.012
Trend (α = 0.05)	none	none	none	none	none

Aggregate annual figure, however, misrepresents the climate trend of the district. The warming is concentrated during the late monsoon period, specifically August (Sen's slope 0.019°C yr^{-1}; p = 0.047) and September (0.029°C yr^{-1}; p = 0.015 under original test). These months are showing significant increase whose combined effects are extending warmer conditions into autumn transition (Figs. 3 and 4). The trend observed in September is a powerful one. It is also one of the strongest in the dataset and, after the Hamed–Rao correction, this trend becomes more significant, not less, ($p < 0.001$). This indicates that it is not merely an artefact of serial correlation. On the contrary, December cools noticeably under the corrected test with a rate of -0.020 °C yr^{-1} and p = 0.018. This result is invisible to the uncorrected Mann-Kendall test and, to our knowledge, was not reported before for this district. For the other months, tau values between −0.133 (June) and 0.193 (February) and p-values > 0.05 confirm the presence of no significant monotonic change; the null hypothesis is retained for these series and rejected only for August, September, and (under the corrected test) December.

Table 3 Mann–Kendall and Sen's slope results for monthly mean temperature, 1990–2024 (bold: significant at α = 0.05 under the Hamed–Rao corrected test)

Month	tau	S	p (orig.)	p (H–R)	Sen (°C yr^{-1})	Trend
Jan	−0.099	−59	0.410	0.410	−0.015	none
Feb	0.193	115	0.105	— [a]	0.038	none
Mar	0.173	103	0.147	0.147	0.047	none
Apr	0.096	57	0.426	0.426	0.027	none
May	−0.099	−59	0.410	0.410	−0.022	none
Jun	−0.133	−79	0.268	0.268	−0.020	none
Jul	0.049	29	0.691	0.691	0.006	none
Aug	**0.237**	**141**	**0.047**	**0.047**	**0.019**	**increasing**
Sep	**0.291**	**173**	**0.015**	**<0.001**	**0.029**	**increasing**
Oct	0.136	81	0.256	0.256	0.017	none
Nov	−0.089	−53	0.460	0.460	−0.008	none
Dec	**−0.187**	**−111**	**0.118**	**0.018**	**−0.020**	**decreasing**

[a] *Variance correction numerically unstable for this series; the original test applies.*

The resulting image is one of seasonal asymmetry instead of uniform warming: A lengthening warm season that persists deeper into September, in conjunction with a sharper, colder onset of early winter. The asymmetry differs significantly from what is seen at higher altitudes. In the northwestern Himalaya, twentieth-century warmth was strongest in winter and driven more by maximum than by minimum temperatures (Bhutiyani et al., 2007). Moreover, recent valley analyses have likewise found winter–spring warming (Zaz et al., 2019; Hamid & Samantaray, 2025); however, the foothill signal detected here occurs in the opposite season. The late monsoon warming mechanism is consistent with the identified weakening of monsoon circulation and cloud cover over northwestern India. As such, this may increase surface insolation during the August-September period, whereas early winter cooling can shift the timing and positions of southern disturbances reported for the region (Krishnan et al., 2020). These designations remain destination hypotheses at the district scale; establishing them would require diagnostics of circulation beyond trend analysis. The temperature anomaly heat map (Fig. 4) visually illustrates this asymmetry: warm anomalies in August–September cluster in the most recent decade, and there is a preponderance of cool anomalies in the December column late in the record.

It is worthwhile to comment on the relation of these findings to that of the only other trend study of the district. According to the analysis of station records from 1985 to 2010, Singh et al. (2021) reported that for Kathua, with shifting monthly rainfall, the annual minimum temperature is rising while the maximum temperature is declining slightly. The present analysis extends over a period of fourteen years and uses a dataset of IMD gridded measurements as opposed to the earlier studies which used station records. Similarly, as opposed to the earlier studies which used the separate maximum and minimum temperatures to calculate a composite, the present study determines the daily mean temperature. This means that while the present study and the earlier study are not directly comparable, they are complementary. However, it is important to note that both studies agree that the thermal change in the district is real, while the rainfall change is unclear. However, the results of the present study localise the thermal signal to specific months in a way that direct comparison cannot. A possible refinement would be to extend the analysis of gridded maximum and minimum temperatures separately to test whether the late-monsoon warming detected here is driven by minimum temperatures, as an asymmetric global pattern would suggest.

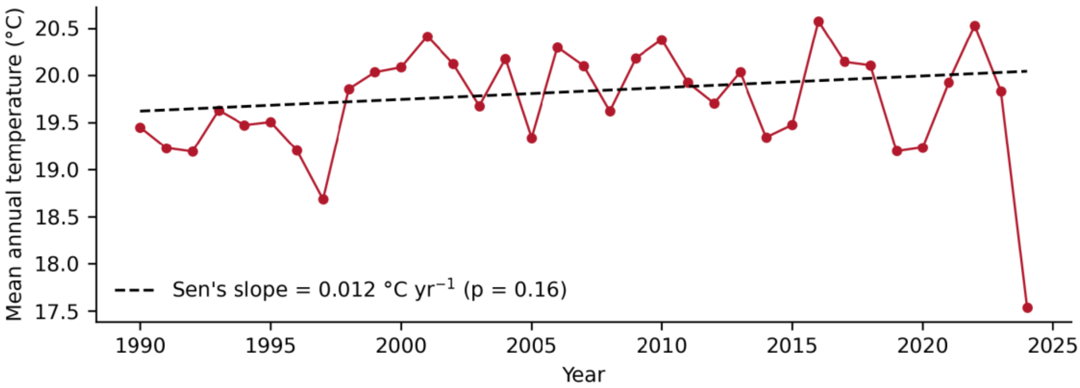

Fig. 2 Annual mean temperature for Kathua district, [1990–2024], with the Theil–Sen trend line. Sen's slope = +0.012 °C yr^{-1} (modified Mann–Kendall, p = 0.16).

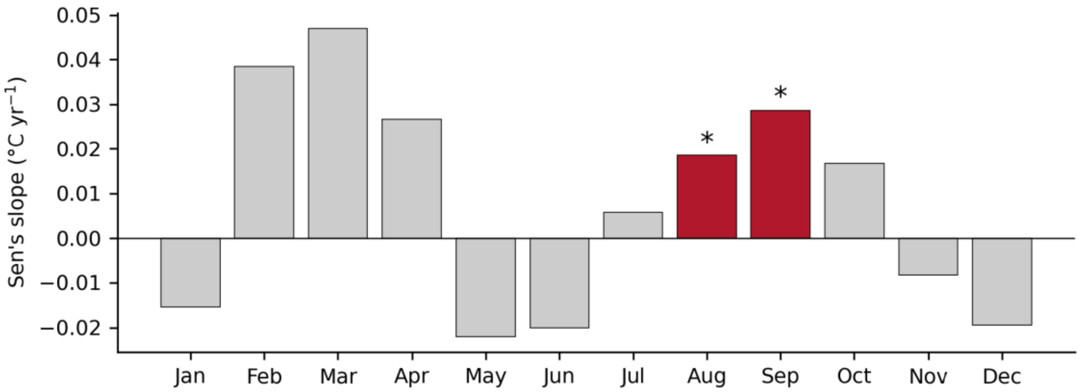

Fig. 3 Month-wise Theil–Sen slopes of mean temperature, [1990–2024]. Asterisks denote months significant at $p < 0.05$ under the modified Mann–Kendall test.

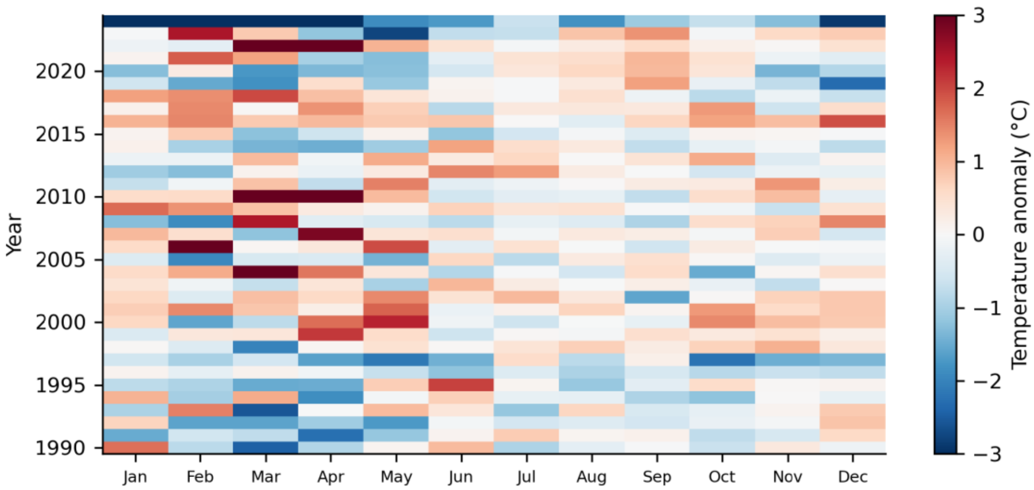

Fig. 4 Monthly mean temperature anomalies (°C, relative to 1990–2024 monthly means), Kathua district

Rainfall

The mean annual rainfall during 1990–2024 is 1,417mm, of which the monsoon (June– September) contributes 62%, while the winter (December–February) adds a further 18%. This rainfall pattern reflects the dual precipitation regime in the Shiwalik foothills, where both summer monsoon depressions and winter western disturbances significantly contribute to the annual water budget, as observed at other foothill locations. The wettest months of the year are July (306 mm) and August (328 mm). The driest months are October and November (≤ 29 mm).

Table 4 Descriptive statistics of monthly, seasonal, and annual rainfall (mm), Kathua district average, 1990–2024

Period	Min	Max	Mean	SD	CV (%)
January	1.7	232.1	91.9	62.6	68
February	11.6	252.2	120.2	71.9	60
March	2.1	274.5	104.3	73.2	70
April	5.7	166.9	69.1	43.7	63
May	13.1	132.9	57.3	22.0	38
June	30.7	347.3	113.0	59.3	52
July	74.9	557.5	305.8	117.1	38
August	124.6	597.3	327.6	136.7	42
September	37.4	315.6	137.6	64.2	47
October	0.0	89.3	28.5	28.8	101
November	0.0	106.1	22.0	28.3	129
December	0.0	209.6	39.7	45.1	114
Winter (DJF)	61	475	252	103	41
Summer (MAM)	92	413	231	95	41
Monsoon (JJAS)	392	1,362	884	230	26
Post-monsoon (ON)	3	179	50	43	86
Annual	785	1,886	1,417	277	19.5

In either the original or autocorrelation-corrected Mann-Kendall test, no monthly, seasonal or annual rainfall series shows a statistically significant monotonic trend. The annual trend is weakly negative (Sen's slope –3.9 mm yr-1; $p = 0.570$; Fig. 5), which is in the same direction as the long-term decline in monsoon precipitation seen in the northwestern Himalaya (Bhutiyani et al., 2010), as well as the decline in winter rainfall documented for the wider Jammu and Kashmir region (Guhathakurta & Rajeevan, 2008). The weakening of the mean monsoon over India (Krishnan et al., 2020) shows the same trend. At this record length, however, it is indistinguishable from natural variability.

Natural Resources for
Human Health
eISSN: 2583-1194

Table 5 Mann–Kendall and Sen's slope results for rainfall, 1990–2024 (no series significant at α = 0.05 under either test)

Series	tau	S	p (orig.)	p (H–R)	Sen (mm yr^{-1})
Jan	0.005	3	0.977	0.977	0.00
Feb	−0.126	−75	0.293	0.293	−1.45
Mar	−0.039	−23	0.755	0.783	−0.39
Apr	0.126	75	0.293	0.288	1.03
May	0.187	111	0.118	0.118	0.53
Jun	−0.022	−13	0.865	0.865	−0.12
Jul	0.072	43	0.551	0.551	1.40
Aug	−0.096	−57	0.426	0.426	−1.53
Sep	−0.119	−71	0.320	0.209	−1.05
Oct	0.097	58	0.418	0.235	0.29
Nov	0.059	35	0.629	0.629	0.11
Dec	0.087	52	0.469	0.408	0.23
Winter	−0.089	−53	0.460	0.460	−0.91
Summer	0.062	37	0.609	0.609	0.79
Monsoon	−0.079	−47	0.514	0.184	−2.42
Post-monsoon	0.150	89	0.211	0.211	0.85
Annual	−0.069	−41	0.570	0.570	−3.86

The lack of a trend does not imply a lack of risk. There has been substantial interannual variability in the data: the annual totals have ranged from 785mm in 2002, when the well-documented all-India monsoon failed, to 1886mm in 1995. Further, the three driest years of the record (2000-2002, all below 980 mm) have been consecutive years (Figs. 5 and 6). A great deal of variability takes place on a monthly basis. The coefficients of variation range between 38% (May, July) and 129% (November). The months following the monsoon and early winter are the least reliable parts of the annual cycle. Thus, unreliable rainfall in any month and recurrent multi-year deficits are the operative climate risks for the district's rain-fed agriculture, not any long-term drying or wetting. As shown in the monthly heat map (Fig. 6), the monsoon core appears as a persistent high-rainfall band with strong year-to-year modulation, with no visual drift in either the onset or withdrawal columns, consistent with the statistical results.

Beyond agriculture, the two-pronged precipitation regime has implications for water resources. Winter precipitation that occurs due to western disturbances supports rabi growing, groundwater recharge, and the Ujh and Sewa river baseflow in the dry pre-monsoon; the weak negative winter trend detected here (–0.91 mm yr^{-1}, $p = 0.460$), though non-significant, is directionally consistent with the regional decline in western disturbance precipitation (Guhathakurta & Rajeevan, 2008) and projections of further weakening with warming (Krishnan et al., 2020) and should therefore be monitored rather than dismissed. On the other hand, since 62% of annual rainfall falls within a four-month monsoon season with a monthly coefficient of variation near 40%, the problem of storage and supply that any water security intervention in the district must resolve is as follows: abundance and deficit are separated by weeks, not by seasons, and years whose ordering trend statistics show to be effectively unpredictable at this record length.

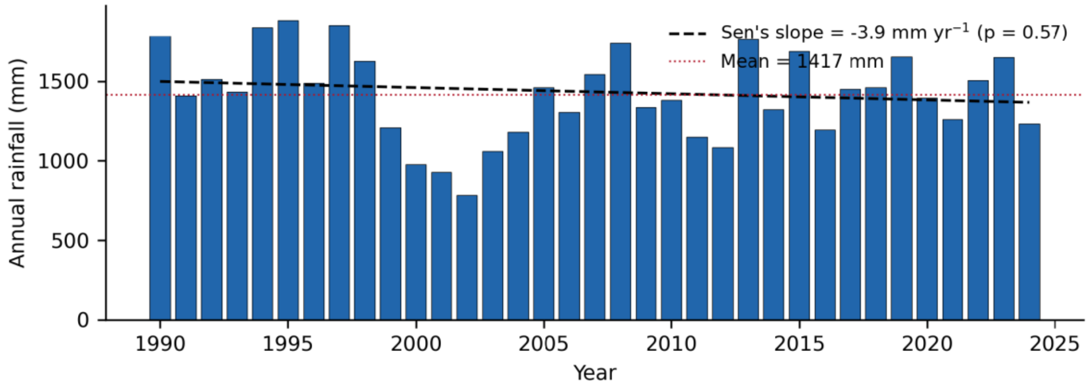

Fig. 5 Annual rainfall for Kathua district, [1990–2024], with long-term mean (dashed) and Theil–Sen trend. Sen's slope = −3.9 mm yr^{-1} (p = 0.57); mean = 1417 mm; coefficient of variation = 19.6%; lag-1 autocorrelation = +0.41.

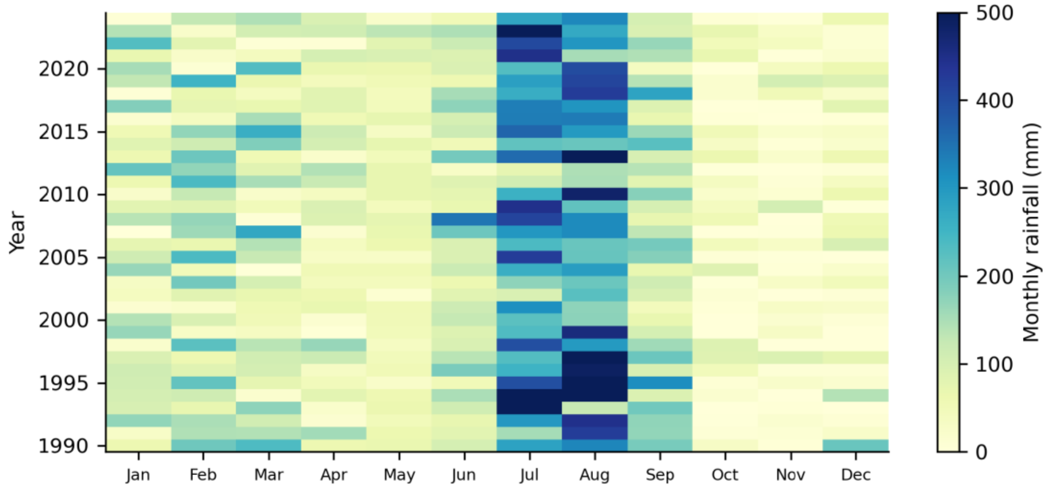

Fig. 6 Monthly rainfall totals (mm), Kathua district average, 1990–2024

Livelihood Implications

The documented seasonal asymmetry directly corresponds to the district's livelihood calendar, and it is here that the statistical findings obtain their geographic significance. The notable increase in temperature during August-September corresponds with the period of fertilisation and harvest of kharif paddy and maize. As a result, heat stress reduces yield and hastens evaporation as monsoon withdrawal takes hold. Due to similar weeks of the fodder availability on the migration routes, the Bakarwal households descend from the high pastures. A longer, warmer autumn transition not only affects the timing of descent but also the condition of arriving herds (Mir & Batool, 2022). As December temperatures decline, the window for germination of rabi wheat sown after the post-monsoon becomes compressed, and the risk of cold stress for livestock in the upland blocks of Bani and Basohli rises. Researchers in the western Himalaya conducted perception studies, which found that cultivators identified month-specific changes in hotter harvests and colder winter beginnings as changes they were already becoming accustomed to, and they adjusted sowing dates and varietal choice accordingly (Negi et al., 2017).

Kathua's high interannual variability, but no compensating trend in rainfall, underlines the case for prioritising adaptation to buffer variability rather than responses based on a consistent warming-and-wetting narrative. Here are the three implications.

First, water harvesting and micro-storage in the Ujh and Sewa catchments respond more directly to the documented recurrence of consecutive deficit years than to supply augmentation. Second, the district's weather-indexed crop insurance should be calibrated to late-monsoon heat exposure as much as to rainfall deficit, since the climate change detected here is thermal and seasonal, not pluvial. Third, guiding farm advisers, alongside designing pastoral routes, should be seen as a moving target in relation to the autumn transition. In other words, calendars should not be based on climatological normals but rather on recent observations. District-level trend detection, robust against autocorrelation, has the potential to make direct contributions to policy initiatives of concerned authorities.

LIMITATIONS

These findings are qualified by four limitations. Initially, the temperature arises from a single grid cell of 1°. At this resolution, the elevation contrasts within the sub-district between the Hiranagar plains and the Bani uplands are unresolved, and the series is better interpreted as the district-average lowland-weighted signal. Moreover, the IMD gridded products derived in mountainous terrains inherit the shortcomings of the station network. While at high elevation the station density is quite sparse, gridded and station datasets can diverge within the northwestern Himalaya. Hence, the trends reported here should be read alongside station-based evidence, if available. The report also examines monotonic trends in means; it does not test extreme indices (e.g., warm spell duration or daily rainfall intensity), which can change considerably even if means are stationary (IPCC, 2021). The detectability of weak trends is limited by the 35-year record due to high interannual variability, particularly in rainfall, where a longer series or stronger signal is required for standardised test confidence in rejecting the null hypothesis. A natural methodological next step would be to extend the analysis to daily extremes, to grid-cell-wise spatial trend mapping, and to formal change-point detection.

CONCLUSION

Between 1990-2024, Kathua district has not experienced uniform climate change but a redistribution of warmth through the seasonal cycle: significant late-monsoon warming (August +0.019 °C yr^{-1}, $p = 0.047$; September +0.029 °C yr^{-1}, $p < 0.001$ under the autocorrelation-corrected test), significant early-winter cooling (December –0.020 °C yr^{-1}, $p=0.018$ under the corrected test), and no significant change in annual mean temperature (+0.012 °C yr^{-1}, $p=0.164$) or in rainfall at any timescale. Interannual variability (including multiple deficit years in 2000–2002) rather than trend dominated annual rainfall (mean 1417 mm; CV 19.5%). The divergence between the original and Hamed–Rao results for September and December reveals that autocorrelation correction is not a mere formality in series at the district scale: it both strengthens a true signal and reveals one that the uncorrected test misses.

The conclusion of practical relevance is that climate risk in this Himalayan foothill district is seasonal and variability-driven; adaptation planning keyed to annual averages will misallocate effort. The late-season warming disrupts weeks on either end of the agricultural and pastoral calendar, while early winter cooling disrupts the establishment phase of the rabi season. At the same time, water security remains constrained by recurring multi-year rainfall deficits. The next logical direction of research in this data-sparse but densely inhabited zone of the Himalayan foothills is household-level evidence on how agrarian and pastoral communities perceive and respond to the late-monsoon shift, along with trend analysis based on extremes and spatially explicit analysis.

Data Availability Statement: The IMD gridded temperature and rainfall datasets analysed in this study are publicly available from the India Meteorological Department, Pune, and were accessed via the open-source IMDLIB library (https://github.com/iamsaswata/imdlib). Processed district-level series are available from the corresponding author on reasonable request.

REFERENCES

[1] Bhutiyani, M.R., Kale, V.S. & Pawar, N.J. Long-term trends in maximum, minimum and mean annual air temperatures across the Northwestern Himalaya during the twentieth century. *Climatic Change* 85, 159–177 (2007). https://doi.org/10.1007/s10584-006-9196-1.

[2] Bhutiyani, M. R., Kale, V. S., & Pawar, N. J. (2010). Climate change and the precipitation variations in the northwestern Himalaya: 1866–2006. *International Journal of Climatology*, *30*(4), 535–548. https://doi.org/10.1002/joc.1920.

[3] Census of India. (2011). *District census handbook: Kathua, Jammu & Kashmir (Series-02, Part XII-A & B)*. Directorate of Census Operations, Jammu & Kashmir.

[4] Dad, J. M., Muslim, M., Rashid, I., Rashid, I., & Reshi, Z. A. (2021). Time series analysis of climate variability and trends in Kashmir Himalaya. *Ecological Indicators*, *126*, 107690. https://doi.org/10.1016/j.ecolind.2021.107690.

[5] Guhathakurta, P., & Rajeevan, M. (2008). Trends in the rainfall pattern over India. *International Journal of Climatology*, *28*(11), 1453–1469. https://doi.org/10.1002/joc.1640.

[6] Hamed, K. H., & Rao, A. R. (1998). A modified Mann–Kendall trend test for autocorrelated data. *Journal of Hydrology*, 204(1–4), 182–196. https://doi.org/10.1016/S0022-1694(97)00125-X

[7] ICIMOD. (2023). *Water, ice, society, and ecosystems in the Hindu Kush Himalaya: An outlook*. International Centre for Integrated Mountain Development. https://doi.org/10.53055/ICIMOD.1028

[8] Immerzeel, W. W., Lutz, A. F., Andrade, M., Bahl, A., Biemans, H., Bolch, T., Hyde, S., Brumby, S., Davies, B. J., Elmore, A. C., Emmer, A., Feng, M., Fernández, A., Haritashya, U., Kargel, J. S., Koppes, M., Kraaijenbrink, P. D. A., Kulkarni, A. V., Mayewski, P. A., … Baillie, J. E. M. (2020). Importance and vulnerability of the world's water towers. *Nature*, *577*(7790), 364–369. https://doi.org/10.1038/s41586-019-1822-y

[9] Intergovernmental Panel on Climate Change (IPCC). (2023). *Climate Change 2021 – The Physical Science Basis: Working Group I Contribution to the Sixth Assessment Report of the Intergovernmental Panel on Climate Change*. Cambridge: Cambridge University Press.

[10] Jaswal, A. K., & Rao, G. S. P. (2010). Recent trends in meteorological parameters over Jammu and Kashmir. *MAUSAM*, *61*(3), 369–382. https://doi.org/10.54302/mausam.v61i3.839.

[11] Kendall, M. G. (1975). Rank correlation methods (4th ed.). Charles Griffin, London.

[12] Krishnan, R., Sanjay, J., Gnanaseelan, C., Mujumdar, M., Kulkarni, A., & Chakraborty, S. (Eds.). (2020). *Assessment of climate change over the indian region: A report of the ministry of earth sciences (Moes), government of india*. Springer Singapore. https://doi.org/10.1007/978-981-15-4327-2

[13] Mann, H. B. (1945). Nonparametric tests against trend. *Econometrica*, *13*(3), 245. https://doi.org/10.2307/1907187.

[14] Mir, S. A., & Batool, M. (2022). Impact of climate change on gujjar and bakarwal communities of jammu and kashmir. *Journal of Sustainability and Environmental Management*, *1*(2), 99–104. https://doi.org/10.3126/josem.v1i2.45342.

[15] Nandi, S., Patel, P., & Swain, S. (2024). IMDLIB: An open-source library for retrieval, processing and spatiotemporal exploratory assessments of gridded meteorological observation datasets over India. *Environmental Modelling & Software*, *171*, 105869. https://doi.org/10.1016/j.envsoft.2023.105869

[16] Negi, G. C. S., Samal, P. K., Kuniyal, J. C., Kothyari, B. P., Sharma, R. K., & Dhyani, P. P. (2012). Impact of climate change on the western Himalayan mountain ecosystems: An overview. *Tropical Ecology*, 53(3), 345–356.

[17] Negi, V. S., Maikhuri, R. K., Pharswan, D., Thakur, S., & Dhyani, P. P. (2017). Climate change impact in the Western Himalaya: People's perception and adaptive strategies. *Journal of Mountain Science*, *14*(2), 403–416. https://doi.org/10.1007/s11629-015-3814-1.

[18] Pai, D. S., Rajeevan, M., Sreejith, O. P., Mukhopadhyay, B., & Satbha, N. S. (2014). Development of a new high spatial resolution (0.25° × 0.25°) long period (1901-2010) daily gridded rainfall data set over India and its comparison with existing data sets over the region. *MAUSAM*, *65*(1), 1–18. https://doi.org/10.54302/mausam.v65i1.851.

[19] Hamid, H., & Samantaray, S. (2025). Spatial and temporal dynamics of climate in Kashmir: A statistical approach to temperature and humidity changes. *ISH Journal of Hydraulic Engineering*, *31*(4), 761–792. https://doi.org/10.1080/09715010.2025.2501966.

[20] Sen, P. K. (1968). Estimates of the Regression Coefficient Based on Kendall's Tau. *Journal of the American Statistical Association*, *63*(324), 1379–1389. https://doi.org/10.1080/01621459.1968.10480934

[21] Singh, M., Sharma, C., Sharma, B. C., & Sharma, R. (2021, March 17–19). Analysis of monthly temperature and rainfall trends for Kathua district of Jammu region [Conference presentation]. V-AGMET 2021, Punjab Agricultural University, Ludhiana. https://doi.org/10.13140/RG.2.2.23086.43848

[22] Srivastava, A. K., Rajeevan, M., & Kshirsagar, S. R. (2009). Development of a high resolution daily gridded temperature data set (1969–2005) for the Indian region. *Atmospheric Science Letters*, *10*(4), 249–254. https://doi.org/10.1002/asl.232

[23] Wester, P., Mishra, A., Mukherji, A., & Shrestha, A. B. (Eds.). (2019). *The hindu kush himalaya assessment: Mountains, climate change, sustainability and people*. Springer International Publishing. https://doi.org/10.1007/978-3-319-92288-1.

[24] Zaz, S. N., Romshoo, S. A., Krishnamoorthy, R. T., & Viswanadhapalli, Y. (2019). Analyses of temperature and precipitation in the Indian Jammu and Kashmir region for the 1980–2016 period: Implications for remote influence and extreme events. *Atmospheric Chemistry and Physics*, *19*(1), 15–37. https://doi.org/10.5194/acp-19-15-2019.